Journal of Applied Polymer Science

# Synthesis of carbazole-substituted poly(dimethylsiloxane) and its improved refractive index

**Norhuda Hidayah Nordin, Mohamad Riduwan Ramli, Nadras Othman, Zulkifli Ahmad**
School of Materials and Mineral Resources Engineering, Universiti Sains Malaysia, Nibong Tebal, Penang, Malaysia
Correspondence to: Z. Ahmad (E-mail: zulkifli@usm.my)

**ABSTRACT:** A series of substituted 9-vinylcarbazole polysiloxane was synthesized followed by room temperature vulcanization to afford a crosslink network via trimethoxysilane crosslinker. Structural confirmation was made using FTIR, one and two-dimensional $^{1}$H- and $^{29}$Si-NMR spectroscopy. Quantitative estimation of the amount of substituted carbazole was made based on NMR data. These were related to the refractive index whose values were in the range of 1.4370–1.4625 at increasing carbazole content. These values are higher than uncrosslink series, attributable to the tightness of the systems. They displayed an improved thermo-optic coefficient compared to linear unsubstituted polydimethylsiloxane (PDMS). The synergistic effect of substituted carbazole unit with the crosslink network of PDMS presents a viable choice of encapsulant for opto-electronic devices. © 2014 Wiley Periodicals, Inc. J. Appl. Polym. Sci. **2015**, *132*, 41654.

**KEYWORDS:** carbazole; crosslinked network; optical properties; polysiloxane; refractive index

Received 9 May 2014; accepted 6 October 2014
**DOI: 10.1002/app.41654**

## INTRODUCTION

Polysiloxane displays several advantages over traditional inorganic glass including flexibility and excellent thermal stability over wide range of temperature, biocompatibility, transparency, significant gas permeability, and good chemical stability. In recent years, several researches on modification of polysiloxane with various substituents were made.[1,2] This included carbazoles having interesting photoconductive and photorefractive properties combined with ease of processing. The aromatic nature of carbazole is known to exhibit high polarizability over a large atomic area which promotes higher refractive indices.[3] Besides, its bulky conjugated aromatic substituent provides good thermal stability and structural rigidity.

Polycondensation and addition reaction form the most common route in designing a new polysiloxane material.[4–7] The synthesis of a series of high MW polysiloxane with pendant carbazole group was reported to involve reaction of poly(hydrogen methylsiloxane) with various $\omega$-alkenylcarbazoles.[4,5] They involved polysiloxane of cyclic structure which were both uncured and cured network. The shortest alkyl spacer group mostly used in these syntheses consisted of three units. It was suggested elsewhere that the general difficulty for substituting any smaller spacer unit of carbazole into polydimethylsiloxane (PDMS) as due to steric hindrance of the fused aromatic rings.[6]

Formation of crosslink network into a structure induces the effect of "densification" with a decrease in free volume.[8] The Lorentz–Lorenz model suggested that the reduction in free volume increased the refractive index (RI). The work of Jin and Zhu[9] showed that crosslink density has an affect on densification during the thermal curing of a polyimide. This led to the initial increase in RI at region 210–280°C followed by a decrease at region 280–350°C due to the thermal degradation process hence resulting in increased free volume. The RI increased again at temperature 350–380°C due to the formation of new crosslink network involving inter-chain crosslinking. A similar trend was observed in our previous work[10,11] on a series of crosslink polysiloxane whose increased in RI was attributed to a reduction in free volume. Coupled with high transparency hence low optical loss of polysiloxane, carbazole substituent would lead to a viable product for use as optoelectronic devices and coatings such as optical sensor,[12] waveguide in circuit board,[13] and LED encapsulants. To the authors' knowledge, no previous work has shown the effect of crosslink network of carbazole substituted polysiloxane particularly its optical properties. This article reported the successful synthesis of a series of polysiloxane by adopting the crosslinking strategy in tuning their refractive

Additional Supporting Information may be found in the online version of this article.

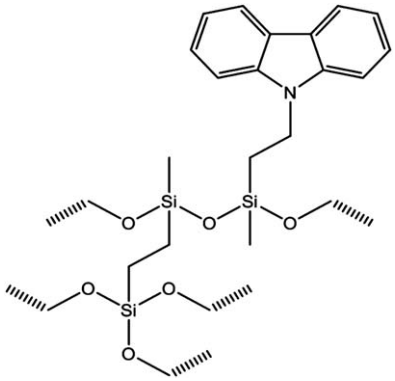

Figure 1. Crosslink network structure of CVS.

indices. Different percentages of pendant carbazole group bearing two methylene spacer units were used. Trialkoxysilane was further introduced as crosslinker to affect an infusible cured product (abbreviated as CVS). The structure of the product is depicted in Figure 1. The optical properties were evaluated based on the amount of pendant carbazole units and were compared to those of uncrosslink series.

## EXPERIMENTAL

### Materials

Octamethylcyclotetrasiloxane ($D_4$), 2,4,6,8-tetramethylcyclotetrasiloxane ($D_4H$), trifluoromethane sulfonic acid (triflic acid), Platinum(0)-1,3-divinyl-1,1,3,3-tetramethyldisiloxane complex (Karstedt's catalyst), 9-vinyl carbazole, and vinyltrimethoxysilane (VTMS) 98% were obtained from Aldrich. Hexamethyldisiloxane was purchased from Aldrich (Germany). The solvents including toluene and ethanol were obtained from J.T. Baker (Germany), which were freshly distilled before use. All other materials were used as received.

### Synthesis

**Synthesis of Poly(dimethyl-*co*-hydromethylsiloxane) Pre-polymer (H-PDMS).** Equilibration reaction was performed using octamethylcyclotetrasiloxane ($D_4$), 2,4,6,8-Tetramethylcyclotetrasiloxane ($D_4H$) (1 mL), hexamethyldisiloxane according to the procedure as in literature.[7] ATR-FTIR ($cm^{-1}$): 2963, 2905, 2154, 1412, 1258, 1062, 1011, 911, 864, 787, 699. $^1$H-NMR ($CDCl_3$, 500MHz) $\delta$, ppm: 4.7 (s, 1H, Si***H***); 0.1–0.05 (m, Si-C***H***$_3$).

**Preparation of Carbazole-VTMS Substituted H-PDMS (CVS).** H-PDMS (3 g, 17.08 mmol), toluene (3 mL), and Karstedt's catalyst (0.0018 mmol, 600 ppm) were charged into a 50 mL two neck round-bottomed flask equipped with dropping funnel. 9-Vinyl Carbazole (wt % based on H-PDMS pre-polymer) was dropped slowly into the reaction mixture. The temperature was increased to 120°C and allowed to react for 3 h with subsequent decrease to 60°C. VTMS was then dropped slowly and allowed for further reaction overnight. The unreacted monomers and other impurities were extracted over reflux at 80°C for 3 h. The excess of toluene was removed using rotary evaporator at 80°C for 2 h affording a clear viscous fluid. ATR-FTIR ($cm^{-1}$): 3056, 2962, 2905, 2840, 1598, 1486, 1409, 1454, 1331, 1258, 1071, 1012, 910, 860, 788, 725, 691. $^1$H-NMR ($CDCl_3$, 500 MHz) $\delta$, ppm: 0.1 (m, (C***H***$_3$)$_3$-Si,), 0.5 (t, -C***H***$_2$-Si-(OCH$_3$)$_3$,2H) 1.1 (t, Si-C***H***$_2$-,2H) 3.5ppm (s, Si-O-C***H***$_3$,9H), 4.4(t, -N(C***H***$_2$-,2H), 4.65(s, Si-***H***,1H), 7.0–8.0 (m, aromatic carbazole hydrogens,8H).

**Preparation of Crosslinked CVS Films.** Room temperature vulcanization (RTV) was performed to affect condensation reaction between methoxy groups using 1 wt % dibutyltin dilaurate as the catalyst under ambient condition. The fluid sample was uniformly spread in the Teflon mould and was cut using a doctor blade in 50 mm × 15 mm × 3 mm and cured at room temperature for 24 h.

### Analytical Technique

**Characterizations.** Infrared spectra were recorded using the Perkin Elmer Spectrum 2000 Attenuated Total Reflectance (ATR-FTIR) Spectroscopy in the range of 4000–500 $cm^{-1}$ region using 16 scans. Proton ($^1$H-NMR) and COSY NMR were performed on a 500 MHz Bruker UltraShield NMR Spectrometer linked to a computer running WIN-NMR software with $CDCl_3$ as solvent. Tetramethylsilane (TMS) was used as an internal reference. $^{29}$Si-NMR was performed on a 99 MHz Bruker NMR Spectrometer using deuterated benzene as solvent.

**Thermal Properties.** Glass transition temperature ($T_g$), crystalline melting temperature ($T_m$), and crystallization temperature ($T_c$) were determined by differential scanning calorimetry. It was performed using DSC 1 Mettler Toledo apparatus coupled with Mattler Toledo STARe software. The test specimens of weight in the range of 5–10 mg were sealed in 40 $\mu$L aluminum capsules with a hole at lid top. The samples were subjected to thermal cycle from −140 to 100°C with a ramp of 10°C/min for the first heating and held for 3 min. The samples were then cooled to −140°C at the rate of 20°C/min under nitrogen purged. The temperature was equilibrated for 5 min at each turning temperature. The results were taken from the second heat ensuring that all samples had removed thermal history.

**Dynamic Mechanical Analysis.** DMA was performed using Mettler Toledo DMA861 in tensile mode at frequency of 1 Hz, force amplitude of 0.5 N, displacement amplitude of 10 μm. The sample was heated from room temperature until 320°C at heating rate of 5°C/min.

Table I. Formulation and Material Designation for Cured and Uncured CVS Series

| Samples | Carbazole contents (wt %) | Concentration (mmol) | | |
|---|---|---|---|---|
| | | Polysiloxane | Carbazole | VTMS |
| H-PDMS | 0% | 18.98 | 0 | 0 |
| S1 | 5% | 18.98 | 0.77 | 1.012 |
| S1u | | 18.98 | 0.77 | - |
| S2 | 10% | 18.98 | 1.55 | 1.012 |
| S2u | | 18.98 | 1.55 | - |
| S3 | 15% | 18.98 | 2.33 | 1.012 |
| S3u | | 18.98 | 2.33 | - |
| S4 | 20% | 18.98 | 3.10 | 1.012 |
| S4u | | 18.98 | 3.10 | - |

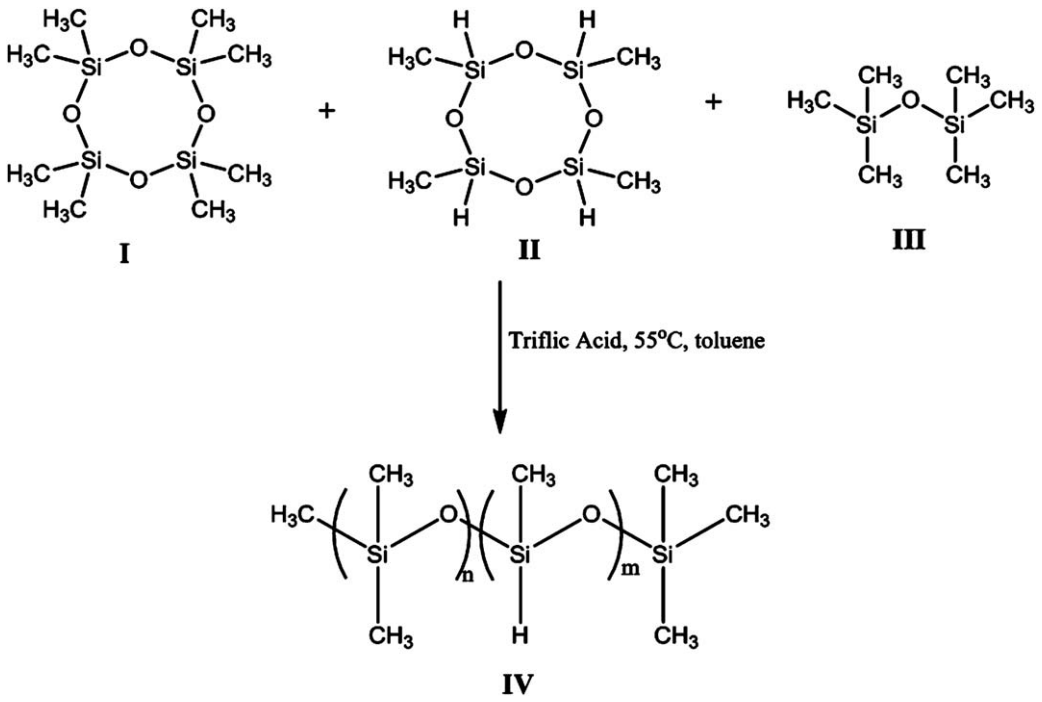


**Scheme 1.** Synthetic route for poly(dimethyl-*co*-hydromethylsiloxane) produced.

**Optical Properties.** The refractive indices were measured using an Abbe refractometer NAR-1T SOLID from Atago Company equipped with circulating constant temperature bath. A drop of monobromonaphthalene was used as the contact liquid between sample and the prism surface. The RI of the samples was taken in triplicate at 25°C, 30°C, 35°C, and 40°C. Monochromatic light source from sodium lamp with 589 nm wavelength was used.

**Degree of Crosslink Network.** The degree of crosslink network was calculated based on the swelling test in toluene for 120 h. The degree of swelling was determined according to eq. (1)[14]:

$$Q=\left[\frac{W_2-W_1}{\rho_S}+\frac{W_1}{\rho_e}\right]\frac{\rho_e}{W1}, \quad (1)$$

where $\rho_{\text{solvents}}$ (toluene) is 0.8669 g/mL, $\rho_e$ is the density of the sample, $W_1$ is weight of the dry sample, and $W_2$ is the weight of swollen sample. The density of the sample was measured using pycnometer. The crosslink density ($X$) was calculated based on Flory–Rehner's eq. (2).

$$X=\frac{-\left[v_2+v_2{}^2x1+\ln\left(1-v_2\right)\right]}{V_1\left(v_2^{1/3}-0.5v_2\right)}, \quad (2)$$

where $v_2$ corresponds to the polymeric volume fraction in swollen mass, $V_1$ is the solvent molar volume, and $x_1$ is the Flory–Huggins polymer–solvent interaction coefficient. The estimated $x_1$ value for PDMS–toluene is 0.465.[15] Meanwhile, the number average molecular weight between the crosslink was determined using eq. (3).[16]

$$\bar{M}c=\frac{1}{X}. \quad (3)$$

## RESULT AND DISCUSSION

### Synthesis of Carbazole-Vinyltrimethoxysilane Polysiloxane

A series of carbazole-vinyltrimethoxysilane polysiloxane (CVS) was produced based on the formulation as shown in the following Table I:

The cured product has used VTMS as a crosslinker. They were fabricated following three stages. The first stage was the preparation of the polysiloxane backbone bearing hydrosilyl hydrogen as the side reactive group. This was followed by substitution by hydrosilylation reaction of both vinyl carbazole and vinyl trimethoxysilane. Finally RTV was performed to afford the cured product. The first stage involved cationic ring opening of $D_4$ and $D_4H$ using triflic acid as the catalyst. The linear polysiloxane was produced as depicted in Scheme 1 below:

Acid catalyst was preferred as the base catalyst as the former gives less cyclic by-products.[17] The amount of $D_4H$ incorporated during ring opening step was made to be in mole excess of 2 : 1 to that of carbazole. This is to ensure a complete substitution of carbazole and VTMS substituents as proven later in H-NMR analysis. The end-capper hexamethyldisiloxane was held at constant mol ratio throughout the preparation so as to maintain the molecular weight of the linear products. In the following step, carbazole and VTMS were substituted onto the polysiloxane backbone through hydrosilylation reaction. The reaction scheme is depicted in Scheme 2.

It was imperative to control the reaction temperature precisely at this step as it influenced the transparency of the synthesized product. This was performed by adding the carbazole and the vinyltrimethoxysilane consecutively at temperature 120°C and 60°C. Because of steric reason, the carbazole with a rigid and

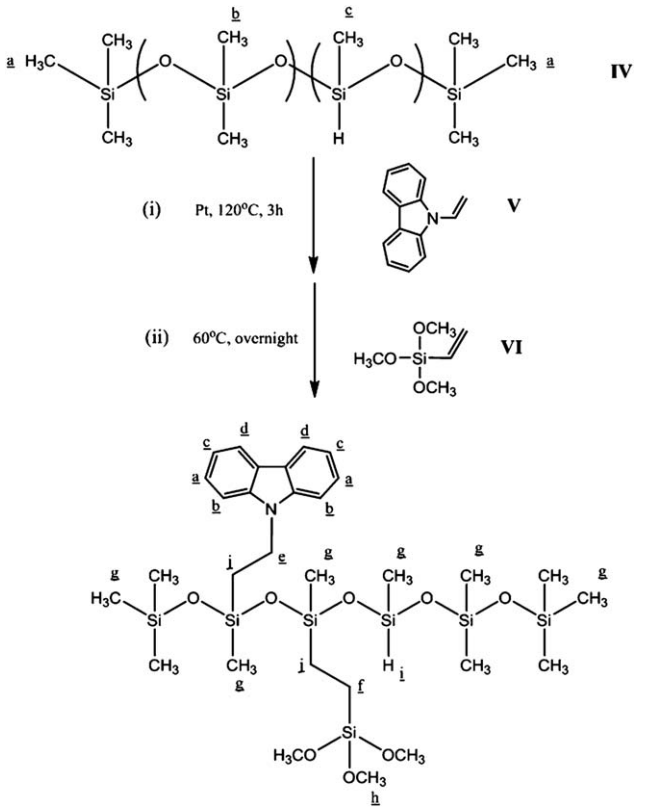


**Scheme 2.** Synthetic route for carbazole-VTMS substitution product (CVS).

bulky structure was added first, followed by a more flexible and loose conformation of vinyltrimethoxysilane. Unreacted substituent monomers were exhaustively extracted under reflux using ethanol. Dry atmosphere was maintained throughout this step to prevent any pre-curing of the product. Once this was established, curing was performed using room temperature vulcanization which involved condensation reaction between methoxy groups of substituted vinyltrimethoxy silane in the presence of dibutyltin dilaurate as the catalyst. The alternative method of using acid catalyst to induce the crosslink structure via hydrolysis/condensation reaction resulted in formation of bubbles in the thin film. This could possibly be the result of the entrapped gaseous product due to an accelerating effect on the rate of reaction. The novelty of the synthetic protocol used in this work demonstrated the use of trimethoxysilane as a versatile crosslinking agent accomplishable at room temperature curing. The tri-functionality of the pendant methoxysilane group afforded not only a ladder-like crosslink network between polysiloxane chains but also intramolecular cyclization of this group yielding mixture of silsesquioxanes, having 12–18 Si atoms made up of complete and incomplete cage-like structures. These assertions will be discussed in the following sections.

### Spectroscopic Identification of Products

Figure 2 showed the FTIR spectra for the polysiloxane before and after carbazole-VTMS substitution. In Figure 2(a), peaks at 2156 $cm^{-1}$ and 910 $cm^{-1}$ are assignable to Si—H group.[9]

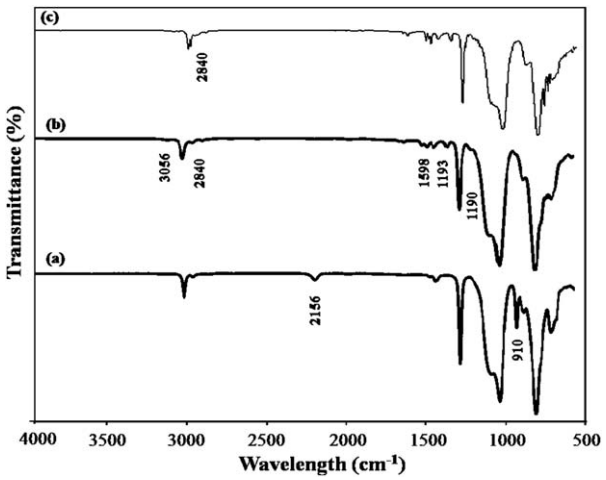


**Figure 2.** FTIR spectra of (a) H-PDMS, (b) CVS with 10 wt % of carbazole substitution before curing, (c) CVS with 10 wt % of carbazole substitution after curing.

The $^1$H-NMR spectrum in Figure 3 of this sample substantiated further the presence of this group with the singlet peak occurring at 4.78 ppm (assigned as **c** in Figure 3). No other peaks occurred in this spectrum except at the region 0.10–0.00 ppm representing the methyl hydrogen attached to the polysiloxane chain backbone.[18]

According to Figure 2(b), the successful substitution of carbazole-VTMS into the polysiloxane was established with the disappearance of the Si—H peak and the corresponding formation of peaks at 3056 $cm^{-1}$ and 1600 $cm^{-1}$ representing the aromatic system of carbazole units. These latter peaks remained in spectrum 2c. The successful substitution of trimethoxysilane into the system is further represented with the formation of a new peak at 2840 $cm^{-1}$ corresponding to the C—H vibration of methoxy group.[19,20] This peak is still visible albeit diminishing intensity in spectrum 2c. The latter observation revealed that not all methoxy groups from the grafted VTMS were hydrolyzed and involved in curing. This observation might be due to the increasing network rigidity with the progress of crosslinking which limited free diffusion and chain movement. This led to the formation of ladder-like or randomly arranged cyclic structure. Several works identified that the two peaks both at regions 1100–1050 $cm^{-1}$ represent the occurrence of closed or partially closed

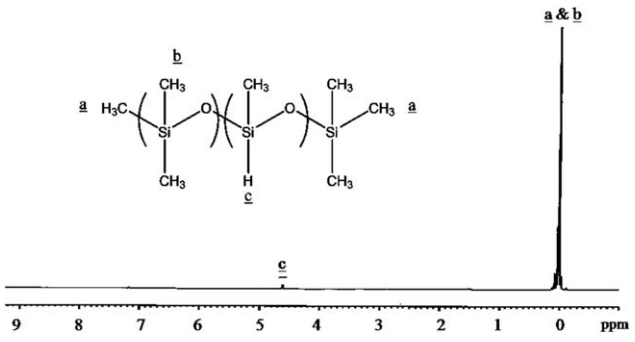


**Figure 3.** $^1$H-NMR spectrum of pendant PDMS.

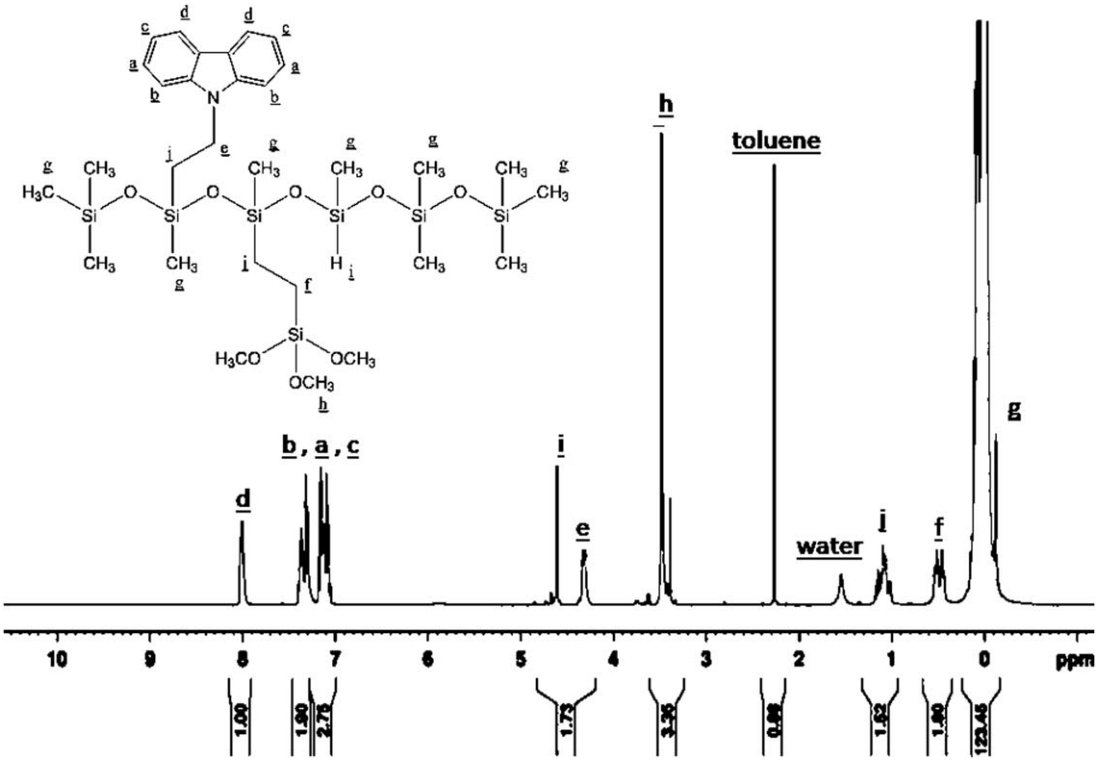


**Figure 4.** [1]H-NMR spectrum of PDMS with carbazole substitution.

caged and the ladder-like or randomly arranged structure, respectively.[21,22] It is noted that peak at 2156 $cm^{-1}$ representing the Si—H appeared in Figure 2(a) but diminished in Figure 2(b,c). Although this represented the consumption of this group during hydrosilylation, it does not imply the total absence of this group in the product *per se*. As proven in *H*-NMR, to be discussed later, this group remained intact possibly at residual level.

The H-NMR spectrum in Figure 4 for carbazole-VTMOS substituted polysiloxane for sample S3 corroborated well with the proposed structure.

The methyl and methylene protons attached directly to the silicone backbone occurred in the region 0–0.2 ppm (designated **g**). The methylene proton at α-position of carbazole unit occurred at 4.3 ppm considerably downfield due to proximity to electronegative nitrogen (designated **e**).[15] Proton at *β*-position of this unit occurred at 1.1 ppm (designated **j**). This is consistent with the COSY spectrum in Figure 5 which shows the correlation between these two peaks. The methylene protons at α-position to the trimethoxy silane units, conversely, occurred at 0.5 (designated as **f**). The *β*-methylene protons of this unit occurred at region 1.1 ppm as exemplified by the COSY spectrum. The singlet at 3.5 ppm corresponded with the methoxy hydrogen which

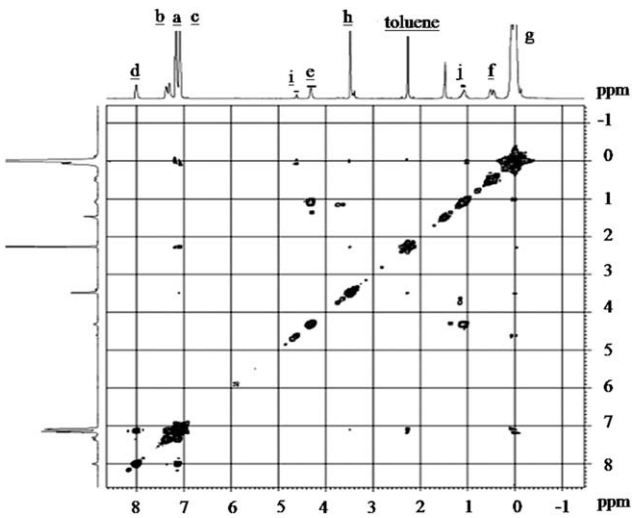


**Figure 5.** 2D [1]H-NMR COSY spectrum of carbazole substituted polysiloxane.

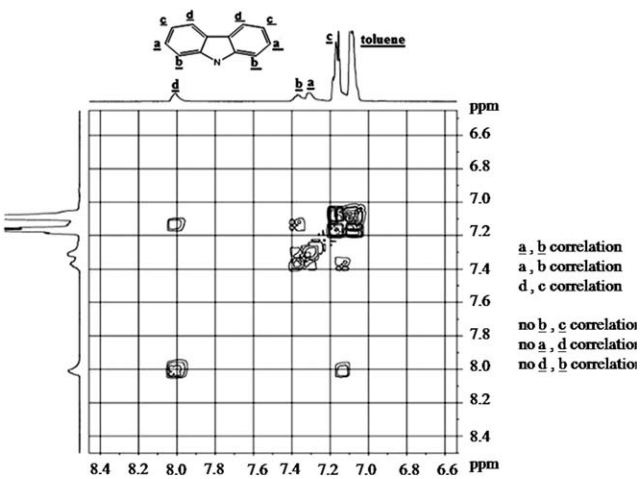


**Figure 6.** Expanded 2D [1]HNMR COSY spectrum for the aromatic region of carbazole substituted polysiloxane.

**Table II.** Quantitative Estimation of the Ratio of Hydrosilyl Proton to the Carbazole Unit of CVS

| Sample designation | Carbazole content (wt %) | Ratio of hydrosilyl proton to the carbazole unit |
|---|---|---|
| H-PDMS | 0 | 0 |
| S1u | 5 | 1.20 |
| S2u | 10 | 0.95 |
| S3u | 15 | 0.81 |
| S4u | 20 | 0.73 |

experienced no coupling with other chemically different neighboring protons (designated **h**). COSY spectrum does not show any significant correlation of these peaks with any others.

There is no peak at 5.0–6.5 ppm which would otherwise correspond to protons of unsaturated carbon derived from either vinyl carbazole or vinyl trimethoxysilane. This significantly proved that the substitution of these groups into the polysiloxane backbone through hydrosilylation is fully accomplished. Compared with FTIR result in Figure 2, residual Si—H groups still remained as observed with the presence of a singlet at 4.6 ppm. This is due to the lower sensitivity of attenuated FTIR whose accessibility of detection is limited on the nanoscale thickness of the sample surface. The expanded COSY spectrum in Figure 6 clearly identified peaks assignment of aromatic ring protons of carbazole unit.

Proton **d** occurred at most downfield at 8.0 ppm as observed in several literature values.[23] Proton **c** occurred at 7.1 ppm which is most upfield of the aromatic protons. This is consistent with the COSY spectrum which shows correlation with the neighboring proton **d**. The peak for the next neighboring proton **b** occurred at 7.3 ppm as confirmed in the correlation in the COSY spectrum. Finally peak at 7.25 ppm corresponded to proton **a** which again showed good correlation to that of proton b. The absence of any correlation of this peak to that of

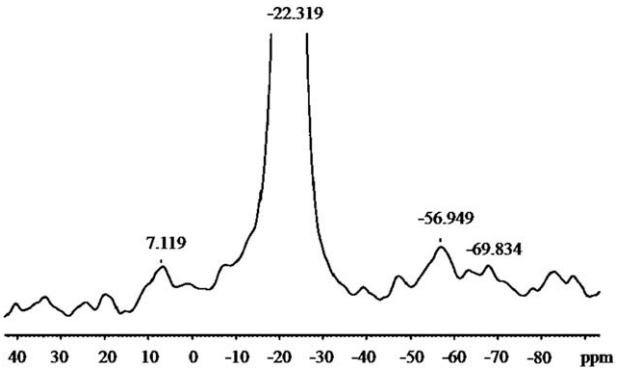


**Figure 7.** $^{29}$Si-NMR spectrum of the PDMS with carbazole substitution.

peak at 7.1 ppm for proton **c** corroborated with this assignment.

Qualitative estimation of the amount of substituted carbazole into polysiloxane can be made based on the NMR spectra. The ratio between hydrosilyl proton at 4.5 ppm to the peak at the aromatic region at 8.0 ppm indicated the amount of carbazole substituted into polymer chain. This is shown in Table II. It can be seen that this ratio reduced as carbazole content increased (see Supporting Information Data for respective NMR spectra; Supporting Information Figure S1–S4).

Figure 7 displayed the $^{29}$Si-NMR spectrum giving information about the type of Si—O—Si bonds present in the substituted PDMS for sample S3. Peak at −22 ppm corresponded with the di-substitution oxygen to siloxane structure (SiO, D) while that at 7 ppm showed the existence of linear siloxane ($SiO_{1/2}$, M) which referred to the end-capper that has been used in the synthesis. The peak at −56 ppm corresponded with the di-substitution oxygen bearing two methoxy group (—$Si(O)_2(OMe)_2$). This has been verified by several works.[24–26] There is a peak of considerable intensity at 69.834 ppm corresponding to the tri-substitution oxygen ($SiO_{3/2}$, T) group.

As with the FTIR analysis, $^{29}$Si-NMR spectrum alone could not confirm whether it is of caged or ladder like structure particularly

**Table III.** Glass Transition and Swelling Parameters for Cured and Uncured CVS Series

| Sample | | $T_g$ (°C) | Number average molecular weight ($cm^3$/mol) | Swelling degree, $Q^*$ |
|---|---|---|---|---|
| Uncured series | HPDMS | −120.2 | - | - |
| | S1u | −115.2 | - | - |
| | S2u | −112.2 | - | - |
| | S3u | −48.8 | - | - |
| | S4u | −37.2 | - | - |
| Cured series | S1 | −83.4 | 180 | 1.38 (0.042) |
| | S2 | −70.0 | 150 | 1.21 (0.021) |
| | S3 | −48.3 | 100 | 1.20 (0.014) |
| | S4 | −10.0 | 95 | 1.18 (0.028) |

*Values in bracket are standard deviation.

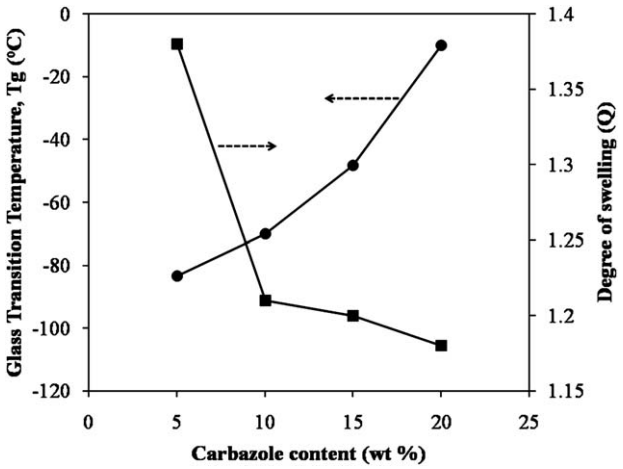


**Figure 8.** The effect of carbazole content on glass transition temperature, $T_g$ and degree of swelling, $Q$.

the cubic $T_8$ silsesquioxane $(R\text{-}SiO_{3/2})_8$.[26] A more rigorous synthetic procedures are needed to afford a pure and high yield $T_8$ polysesquioxane as exemplified in several previous works.[27,28] Based on the preceding spectroscopic analyses, the chain network formation can be envisaged as densely crosslink structure of cyclic and partially cyclic silsesquioxane ($RSiO_{1.5}$), ladder type ($RSiO$, $RSiO_{0\text{-}5}$), with randomly attached carbazole unit either as free pendant group or stacked parallel to each other to form crystalline domain.

### Crosslink Network Properties

The thermal and swelling properties for the cured and the uncured series are shown in the following Table III.

The $T_g$ of the uncured samples increase from −115.14 to −37.20°C with increasing percentage of carbazole content in the PDMS pendant chain. This is due to chain mobility restriction by the bulky carbazole ring. For H-PDMS sample, the $T_g$ occurred at −120.24°C corresponding well with the commonly found unmodified polydimethylsiloxane.[29] Meanwhile, for cured series, the $T_g$ progressively increased to −10.03°C as in sample S4. Several minor and gradual endothermic step transitions were detected over the whole scan corresponding to some localized vibrating motion either at crosslinking point or the carbazole unit. No melting transition was observed in all samples

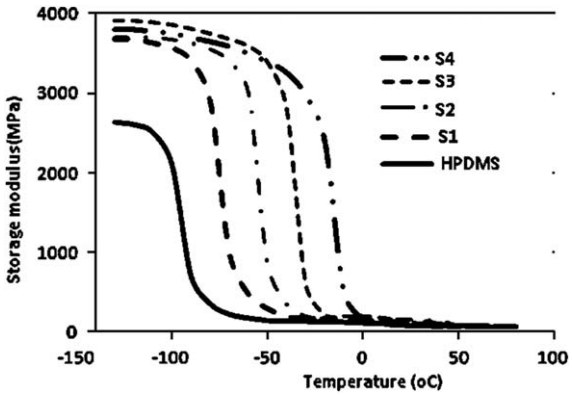


**Figure 9.** Storage modulus with the change in temperature.

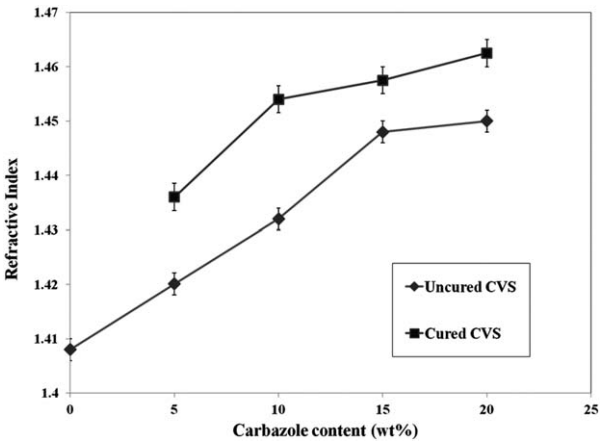


**Figure 10.** RI of cured and uncured CVS.

within the measured temperature range of −130 to 30°C. Swelling test corroborate well to this result which shows a progressive decrease as the carbazole content is increased. The relationship between the glass transition and degree of swelling with the carbazole content is shown in Figure 8.

Based on Flory–Rehner's treatment, swelling test relates to the crosslink density in a network. For uncured series, it resulted in gradual dissolution of the material into the toluene solvent. In the cured system, as it used the same mole concentration of VTMS crosslinker, it is envisaged that with the increase in bulky carbazole content leading to a tight system with a decrease swelling rate. Apparently, with almost constant amount of crosslink network, an increasing amount of substituted carbazole becomes increasingly immobilized. The effect of bulky substituents incorporated into crosslink network has been observed in several system.[26,30,31] Kim *et al.* observed that glass transition is not obviously observed in a crosslink network consisting of bulky POSS structure as due to tightness of this system.[26] This result showed that crosslinking affected chain rigidity and tightness into the network as in the case of thermoset.[11,32] These results were substantiated further through viscoelasticity study of the cured samples using DMA analysis. Figure 9 displays the storage modulus with the change in temperature.

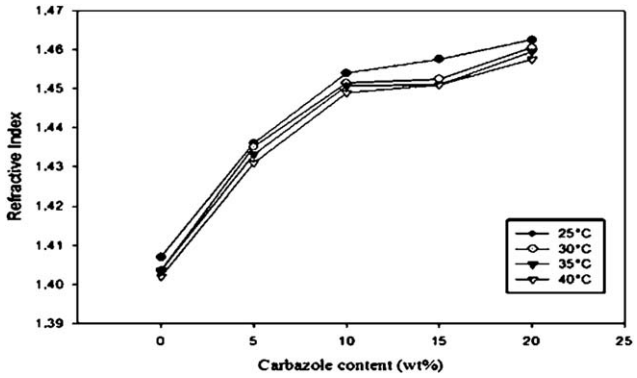


**Figure 11.** Effect of carbazole content on the RI of cured CVS taken at 25, 30, 35, and 40°C.

**Table IV.** Effect of Carbazole Content on the RI of Cured CVS Taken at 25, 30, 35, and 40°C

| | Carbazole content (wt %)[a] | | | | |
|---|---|---|---|---|---|
| Temperature (°C) | 0 | 5 | 10 | 15 | 20 |
| 25 | 1.4073 (5.9) | 1.4361 (7.2) | 1.454 (4.2) | 1.4575 (3.6) | 1.4625 (6.7) |
| 30 | 1.4035 (5.6) | 1.4348 (4.5) | 1.4545 (3.4) | 1.4568 (2.6) | 1.4622 (5.1) |
| 35 | 1.4028 (8.4) | 1.4343 (7.7) | 1.4503 (8.2) | 1.4562 (7.8) | 1.4616 (3.6) |
| 40 | 1.4022 (8.3) | 1.4314 (6.9) | 1.4495 (6.3) | 1.4353 (9.3) | 1.4581 (7.2) |

[a] Values in bracket are std deviation $\times 10^{-4}$.

The sudden drop in the storage modulus for all samples in the region of range −100 to 0°C corresponds to their respective glass transitions. It was noted that these values are slightly higher than those obtained from the DSC result as similarly observed elsewhere.[33] This is due to the different mode of deformation involving the viscoelasticity of the sample used during dynamic testing whereas in DSC it involved changes in heat capacity during thermal changes. All samples containing carbazole substituents display a higher storage modulus compared to that without prior to the onset of glass transition temperature. This occurred due to the presence of bulky and sterically rigid carbazole units between the cross linking points. The number average molecular weight between crosslink points was effectively reduced.[28] This model corroborated well with the defined non-porous material as proposed by Lowman.[34]

## Optical Properties

**Refractive Index.** Figure 10 showed the RI of cured and uncured CVS increases correspondingly with the change in carbazole content.

The sample without carbazole showed RI of 1.408 whose value is comparable to that of commercial Sigma Aldrich sample. For the cured series, the RI increased at least by 2.0% while uncured series 0.92%. These significant observations can be explained based on the Lorentz–Lorenz model, eq. (4),

$$Rm = \frac{n^2-1}{n^2+2}\frac{Mw}{\rho} = \frac{NA\alpha}{3\varepsilon_0}, \quad (4)$$

where $R_m$ is molar refractivity, $\rho$ is density, $\alpha$ is a polarizability, and $\varepsilon_0$ is relative permittivity in vacuum. This equation showed that RI increases with increase in polarizability and density. Carbazole structure is heavily constituted with unsaturated aromatic bond that is highly polarizable.[6] The molar volume of carbazole unit is also large due to the presence of fused tricyclic-ring system. Under the constraint of crosslink network, the system becomes increasingly tight and immobilized with the increase in carbazole content. This results in a reduction in free volume with the concomitant increase in density of the sample. Effectively, the polarizable group per unit volume is increased. The velocity of light that passed through the medium would be reduced leading to the increase of RI. This model that incorporated the significant role of free volume is consistent with the behavior of RI at various temperatures as shown in Figure 11.

The graph showed that over the whole range of carbazole weight content, there was a decrease of RI as the temperature is increased. This is due to the expansion hence increase in free volume with the increase in temperature. This result is summarized in Table IV which includes the standard deviation taken from triplate measurements for each value.

Within these ranges of temperatures, there are an abrupt increase initially followed by saturation beyond 10% carbazole content. This observation can be possibly explained in terms of rate of change of polarizability and free volume. The interplay between these two will determine the net RI. Apparently, the rate of decrease of free volume is slower than the rate of increase in polarizability as due to that of carbazole content. The fact that the result showed a saturation behavior indicated the decrement in rate of free volume change is more dominating as compared to the polarizability factor. Hougham *et al.* has differentiated between these two factors and shown that free volume is a substantial factor in determining the RI.[35] Measurement of thermo-optic coefficient revealed that the cured samples displayed a lower values compared to the uncured series. This was obtained by plotting RI with the change in temperatures. The various values are summarized in the following Figure 12.

It was shown that thermo-optic coefficient is dependent solely on density as given by the following relation in eq. (5):

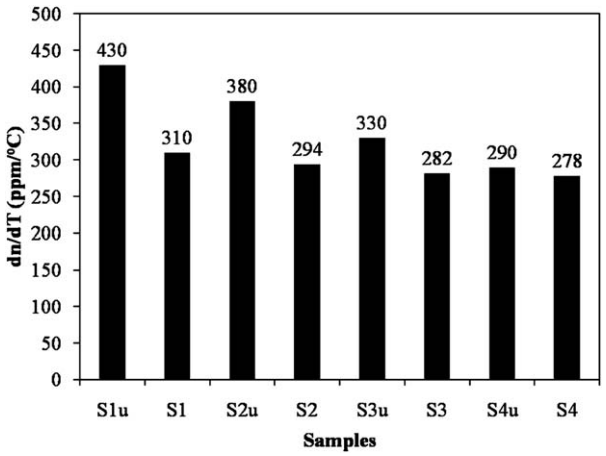


**Figure 12.** Variation of thermo-optic coefficient for cured and uncured series.

$$-\frac{dn}{dT}=\frac{(n^2+2)(n^2-1)}{6n}\frac{1}{\rho}\frac{d\rho}{dT}, \quad (5)$$

where $\frac{1}{\rho}\frac{d\rho}{dT}$ is the volume expansion coefficient.[31,36] The temperature coefficient of the polarizability is almost negligible ($d\alpha/dT \approx 0$). The plot showed that at specified carbazole concentration, the cured series displayed a higher thermo-optic coefficient than the corresponding uncured series. A commercially produced PDMS studied for use as waveguide layer was found as −359 to −365 ppm/°C.[13] The lower thermo-optic coefficient for cured series represented an increase in tightness due to the formation of crosslink network. Thus, the cured series of carbazole-substituted PDMS is better able to retain its RI with the change in temperature. The stability of thermo-optic coefficient in this range of temperature provides a viable material displaying athermal waveguide behavior.

## CONCLUSION

Carbazole substituted of crosslink network polysiloxane was successfully synthesized by cationic ring opening polymerization of $D_4$ followed by hydrosilylation and RTV curing. The increase in carbazole content affected the increased in RI as well as a reduction in thermo-optic coefficient. This is mainly attributed to the high polarizability of carbazole units and the reduction in free volume as the result of crosslink network formation. These observations are consistent with the Lorenz–Lorentz model. The strategy of introducing crosslink network adopted in this work leads to a viable product of tuneable RI and low thermo-optic coefficient for use as PDMS-based optical devices encapsulant.

## ACKNOWLEDGMENTS

Financial support from USM Research University Grant (RU-PRGS 8036013) and the IIUM Fellowship Scheme for NHN is greatly acknowledged.

## REFERENCES

1. Bartlett, I.; Marshall, J.; Maud, J. *J. Non-Cryst. Solids* **1996**, *198*, 665.
2. Wang, W. *Eur. Polym. J.* **2003**, 39, 1117.
3. Seferis, J. C. In Polymer Handbook; Brandrup, J., Immergut, E. H., Grulke, E. S., Eds.; Wiley: New York, **1989**, p 571.
4. Maud, J. M.; Vlahov, A.; Goldie, D. M.; Hepburn, A. R.; Marshall, J. M. *Synth. Met.* **1993**, *55*, 890.
5. Strohriegl, P. *Die Makromol. Chem. Rapid Commun.* **1986**, *7*, 771.
6. Kohjiya, S.; Maeda, K.; Yamashita, S.; Shibata, Y. *J. Mater. Sci.* **1990**, *25*, 3368.
7. Ramli, M. R.; Bisyrul, M. O. H.; Arifin, A.; Ahmad, Z. *Polym. Degrad. Stab.* **2011**, *96*, 2064.
8. Huang, Y.; Paul, D. *Effect of temperature on physical aging of thin glassy polymer films. Macromolecules* **2005**, *38*, 10148.
9. Jin, X.; Zhu, D. *Eur. Polym. J.* **2008**, *44*, 3571.
10. Yahya, S. N.; Lin, C. K.; Ramli, M. R.; Jaafar, M.; Ahmad, Z. *Mater. Des.* **2012**, *47*, 416.
11. Tyng, L. Y.; Ramli, M. R.; Othman, M. B. H.; Ramli, R.; Ishak, Z. A. M.; Ahmad, Z. *Polym. Int.* **2013**, *62*, 382.
12. Zhang, Z.; Zhao, P.; Lin, P.; Sun, F. Thermo-optic coefficients of polymers for optical waveguide applications. *Polymer* **2006**, *47*, 4893.
13. Kopetz, S.; Cai, D.; Rabe, E.; Neyer, A. *AEU-Int. J. Electron. Commun.* **2007**, *61*, 163.
14. Sperling, L. H. Introduction to Physical Polymer Science; Wiley-Interscience: Hoboken, **2005**.
15. Hauser, R. L.; Walker, C.; Kilbourne, F. *Ind. Eng. Chem.* **1956**, *48*, 1202.
16. Thomas, V.; Jayabalan, M. *J. Biomed. Mater. Res A* **2009**, *89*, 192.
17. Chojnowski, J.; Cypryk, M. Synthesis of Linear Polysiloxanes, Silicon-Containing Polymers. The Science and Technology of Their Synthesis and Applications; Kluwer Academic Publishers: Dordrecht, **2000**.
18. Cai, G.; Weber, W. P. *Polymer* **2004**, *45*, 2941.
19. Crompton, T. R. In Organic Silicon Compounds; Patai, S., Rappoport, Z., Eds.; John Wiley & Sons Inc, **1989**, p 393.
20. Smith, A. L. *Spectrochim. Acta* **1960**, *16*, 87.
21. Brown, J. F.; Vogt, L. H. *J. Am. Chem. Soc.* **1965**, *87*, 4313.
22. Ro, H. W.; Park, E. S.; Soles, C. L.; Yoon, D. Y. *Chem. Mater.* **2010**, *22*, 1330.
23. Li, Z.; Li, J.; Qin, J.; Qin, A.; Ye, C. *Polymer* **2005**, *46*, 363.
24. Buestrich, R.; Kahlenberg, F.; Popall, M.; Dannberg, P.; Müller-Fiedler, R.; Rösch, O. *J. Sol-Gel Sci. Technol.* **2001**, *20*, 181.
25. Kim, S. Y.; Augustine, S.; Eo, Y. J.; Bae, B. S.; Woo, S. I.; Kang, J. K. *J. Phys. Chem. B* **2005**, *109*, 9397.
26. Kim, J.-S.; Yang, S.; Bae, B.-S. *Chem. Mater.* **2010**, *22*, 3549.
27. Handke, B.; Jastrzębski, W.; Kwaśny, M.; Klita, Ł. J. Mol. Struct. **2012**, *1028*, 68.
28. Chen, D.; Nie, J.; Yi, S.; Wu, W.; Zhong, Y.; Liao, J.; Huang, C. *Polym. Degrad. Stab.* **2010**, *95*, 618.
29. Kim, G.-D.; Lee, D.-A.; Moon, J.-W.; Kim, J.-D.; Park, J. *Appl. Organomet. Chem.* **1999**, *13*, 361.
30. Nielsen, L. *J. Macromol. Sci. Rev. Macromol. Chem.* **1969**, *C3*, 399.
31. Lee, Y.-J.; Kuo, S.-W.; Huang, C.-F.; Chang, F.-C. *Polymer* **2006**, *47*, 4378.
32. Huang, Y.-J.; Liang, C.-M. *Polymer* **1996**, *37*, 401.
33. Ye, J.; Liang, G.; Gu, A.; Zhang, Z.; Han, J.; Yuan, L. *Polym. Degrad. Stab.* **2013**, *98*, 597.
34. Lowman, A. M. Smart Pharmaceuticals. www.gatewaycoalition.org/files/NewEH/htmls/lowman.doc. (Accessed September 7, 2008).
35. Hougham, G.; Tesoro, G.; Viehbeck, A. *Macromolecules* **1996**, *29*, 3453.
36. Diemeer, M. B. *J. Opt. Mater.* **1998**, *9*, 192.